Performance of a Low-Blowby Sealing System for a High Efficiency Rotary Engine

Maxime Leboeuf and Jean-François Dufault Université de Sherbrooke

Mark Nickerson, Kyle Becker, Alexander Kopache, Nikolay Shkolnik, and Alexander Shkolnik LiquidPiston Inc.

Mathieu Picard Université de Sherbrooke

Abstract

The X engine is a non-Wankel rotary engine that allies high power density and high efficiency by running a high-pressure Atkinson cycle at high speeds. The X engine overcomes the gas leakage issue of the Wankel engine by using two axially-loaded face seals that directly interface with three stationary radially-loaded apex seals per rotor. The direct-interfacing of the apex and face seals eliminates the need for corner seals of the typical Wankel engine, significantly reducing rotary engine blowby. This paper demonstrates the sealing performance that can be achieved by this new type of seal configuration for a rotary engine based on dynamics models and experiments. The dynamics models calculate the displacement and deformation of the face and apex seals for every crank angle using a time implicit solver. The gas leakage is then calculated from the position of the seals and pressure in the chambers and integrated over a rotor revolution. An "effective leakage orifice" area can be determined, to compare blowby between different engine types. Model results show that the X engine equivalent leakage area could be around 35% that of the leakage area of a similarly sized Wankel engine obtained from the same modeling method, which brings the X engine leakage closer to the piston engine's leakage range. Initial experimental results support the findings from the model, as the X engine shows an equivalent leakage area of about 65% that of a scaled Wankel engine. This result demonstrates the potential of the X engine to achieve gas sealing improvements through additional seal development.

Introduction

For applications that need a high power density, the rotary engine has been an interesting candidate since its debut in the 1950s. In addition to its impressive power density, it also features fewer moving parts and lower vibrations levels compared to piston engines. However, it has seen a decrease in popularity in recent years, notably in the automotive industry, with the last remaining Wankel engine powered car being manufactured in 2012. The withdrawal of rotary engines from the automotive market can be explained by the traditional drawbacks of rotary engines, along with increasing emission regulations around the globe.

An important drawback of the rotary engines is the difficulty to seal the combustion chamber. The Wankel engine's geometry requires radially loaded apex seals as well as axially loaded face seals, and the interface between these is not effectively sealed which leads to increased leakage. Various scientific work has been done on the Wankel type rotary engines since the 1950's. The sealing performance of the Wankel engine was studied both experimentally and by modeling. Different methods were used to simulate the Wankel engine by the past, such as modifying piston engines commercial simulation softwares [1], by the use of CFD tools [2], or by analytical calculations [3, 4]. Throughout the literature, the seal leakage values are usually quantified as an equivalent orifice area, which is not directly linked to the dynamics of the seals. This leakage area is usually determined by fitting a full engine cycle simulation model to experimental in-cylinder pressure and other data, tuning parameters such as compression ratio, port flow coefficients, heat transfer multipliers, and leakage orifice areas. For a Mazda Wankel, Eberle and Klomp [5] determined a leakage area value of 2 mm² per cell, while others [6]-[8] found 1 mm².

In an effort to better understand the behavior of the Wankel seals, models were created to study the dynamics of the seals [9]-[12]. The seal model by Picard [3, 4] successfully relates the sealing performance to the dynamics and deformation of the seals to predict leakage. The final results of the model predict an equivalent leakage area varying between 1 mm² and 2 mm² for the Renesis engine. The main conclusion of these studies is that the seals tend to leak near the extremities of the parts that interact with each other. In a piston engine, since the rings only have a single gap, they are able to achieve better sealing performances than Wankel engines.

The X Engine is a rotary engine with an alternative architecture that has the potential to solve the rotary engine sealing

FIGURE 1 The cooling and intake flow enter the engine axially and a mix of exhaust gases and cooling flow exits on the other side
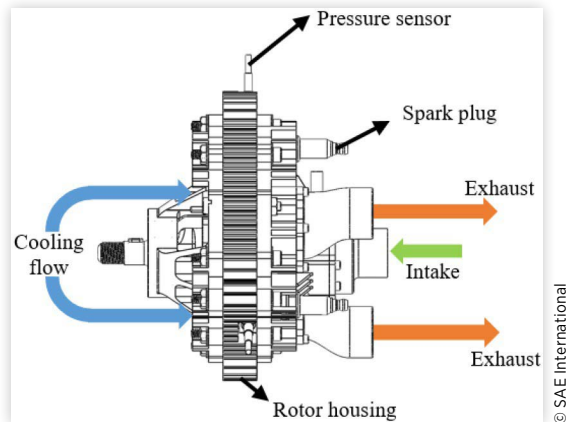

issue by eliminating the need for corner seals. The X engine uses a single face seal each on the front and back rotor periphery. By decreasing the number of interfaces between seals, gaps and potential leakage mechanisms are minimized, which benefits the sealing performance of the engine. The X engine is often described as an "inverted" Wankel engine. Its main particularities are the incorporation of constant volume combustion and over-expansion. A 70 cc version of this engine was manufactured and tested on a dyno and in representative environments [13]. In this 70 cc version, depicted on Figure 1, the intake air comes in through the crankshaft and flows through the rotor to fill each of the three working chambers. As the rotor turns, the intake cavity crosses the apex seals, which opens a flow path between the crankshaft and each working chamber. As the rotation of the rotor continues, the intake port then crosses the apex seal on the other side of the working chamber, which closes the intake air flow path. The gas in the working chamber is then compressed, ignited, and expanded until the exhaust port reaches an apex seal and allows the gases to escape the combustion chamber into the exhaust duct. The main steps of a power stroke are presented in Figure 2.

As the X engine is relatively new, a limited quantity of information has been published on the X engine sealing system. The current literature describes the general architecture of the engine [14, 15], the development of the engine [13] to achieve a working prototype and heat transfer losses predictions and measurement [16]. No previous work on the X engine shows a seal model with the level of details of the ones used for the Wankel or the piston engines.

This paper presents the sealing system of the X engine and an evaluation of its performance. Modeling techniques for the Wankel engine are used to determine the dynamics, deformation, and ultimately the leakage of the seals. Each of the different leakage paths of the working chamber is identified, explained and quantified in order to obtain a final equivalent leakage area value, which is then compared to a scaled Wankel engine. Modeling results show that the X engine's sealing strategy decreases the equivalent leakage area by approximately 65% as compared to a similar sized Wankel engine. The model results are supported by experimental data which shows leakage values of 35% less than the same sized

FIGURE 2 The X engine 4 steps of a power stroke a) Intake b) Compression c) Combustion d) Exhaust
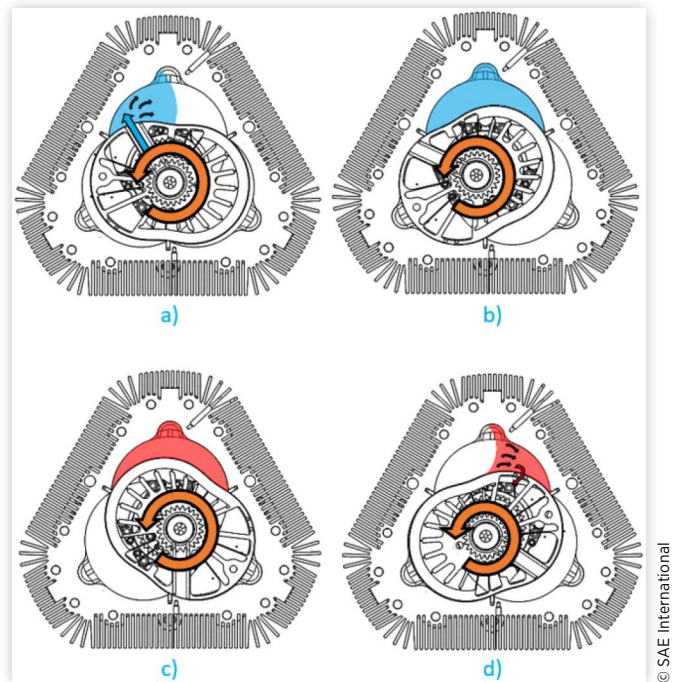
Wankel engine for an engine with less development invested compared to the Wankel engine.

X Engine Sealing System

The X Engine relies on pressure actuated seals shown in Figure 3 to seal the three working chambers. Three apex seals are used to seal between the chambers and two face seals seal the interface between the rotor and the housing plates. The absence of corner seals reduces the number of gaps to seal compared to Wankel engines and therefore tends to increase the sealing performance.
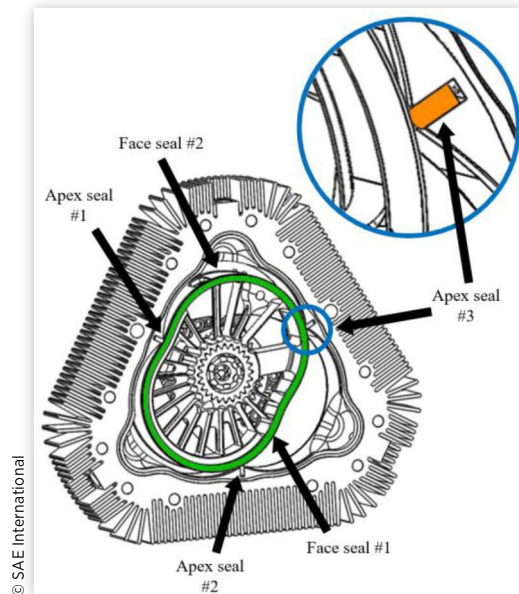
Face Seals

The face seals are located on each side of the rotor and are constituted of two parts, the internal and external face seals. The internal seal is pre-loaded by springs located inside the rotor. It then transfers the spring load uniformly on the external face seal. The external face seal is the key component in the assembly. Mounted on the exterior of the rotor, it prevents high pressure gases in the working chamber from leaking to the atmosphere through its flank and through the running face, as shown on Figure 4. The face seal is activated by the pressure in the working chamber and conforms to both the housing and the rotor, sealing the gaps and preventing pressure losses.

Apex Seals

The apex seals show a design similar to Wankel apex seals, but are stationary on the housing instead of moving with the

FIGURE 3 The X engine features 3 stationary apex seals and 2 face seals


© SAE International

rotor. The apex seal tips therefore run on both the rotor and face seal surfaces. By making them stationary, the seals are not subjected to centrifugal forces, which makes them more stable in the groove. Gaps and seal dimensions are very close to the Wankel engine apex seals. Figure 5 and Figure 6 show the X engine apex seal components.

The apex seals are composed of 4 different parts. The two pieces located at the extremities of the apex seal are called radial pieces. The radial pieces are running on the face seals in order to adjust to the relative motion between the face seals and the rotor. The two remaining pieces are very alike to the Wankel apex seals. The purpose of this 4-parts design is to minimize geometrical leakage by limiting gaps between parts. The four pieces of the apex seal are spring-loaded to ensure constant contact with the running surface and are activated by the working chamber pressure.

FIGURE 4 The face seal running face and flank surfaces prevent leakage between the high pressure chamber and the side of the rotor


© SAE International
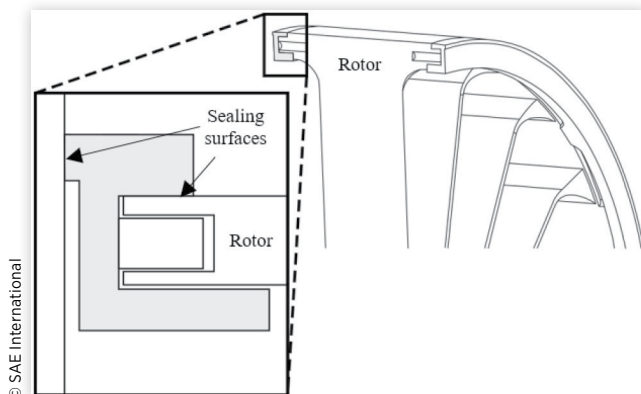
FIGURE 5 The apex seals a) are located on the intersection of each working chamber b) are preventing the gas to flow from one chamber to the other

© SAE International
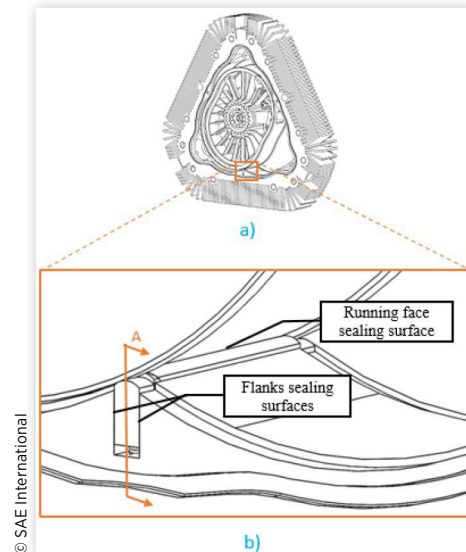
There are three possible leakage paths associated with the apex seals. All three of them are presented in Figure 6. The geometrical leakage area is identified as the gaps between the apex seal parts, which is caused by thermal and mechanical deformations as well as manufacturing tolerances of the parts. Leakage between the rotor and the running face of the apex happens when the forces on the apex are not balanced and the seal separates from the rotor. The leakage between the groove and the apex side happens when the apex seal moves from one side of the groove to the other, under the action of pressure variations. Figure 5 shows the leakage paths related to the dynamics of the apex.

FIGURE 6 The apex seal 4 pieces design goal is to keep the geometrical leakage to a minimum (View A from Figure 5 is depicted)

© SAE International
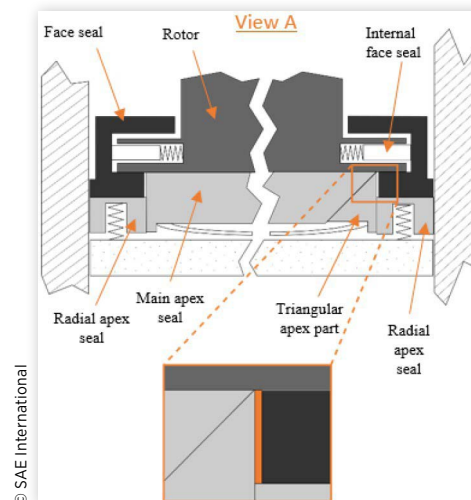
Analytical Development

In order to quantify the leakage performance of the X Engine, models are developed and used for the apex and face seals. The models are based on the modeling strategies previously used by Picard [3, 4] to model the Wankel engine. Both models showed minimal leakage caused by the movement of the X engine seals. The remaining leakage paths are located at the interfaces between the parts.

Apex Seal Model

The X Engine apex seal performance can be evaluated by studying the displacement of the seal in its groove during a complete cycle. To do so, a model solving the rigid-body displacements of the seal for every crank angle is used. The apex seal model aims to quantify two different types of leakage, the flank leakage flow and the running face leakage flow. The flanks leakage is due to the apex moving from one side of the groove to the other and the running face leakage occurs if the apex seal loses contact with the rotor, or if the apex does not conform completely with the rotor due to thermal and mechanical deformations. The position of the rotor and pressure in each chamber for each time step are inputs to the model, which only study the seal itself.

Solver For every crank angle step, the model uses a Newton-Raphson iterative algorithm that minimizes an error function to find an acceptable value for all of the variables comprised in the unknown vector X:

$$X_a = \begin{bmatrix} x_a \\ y_a \\ \phi_a \\ m_g \end{bmatrix}$$

FIGURE 7 Three degrees of freedom are included in the apex seal model: lateral displacement, radial displacement and tilt
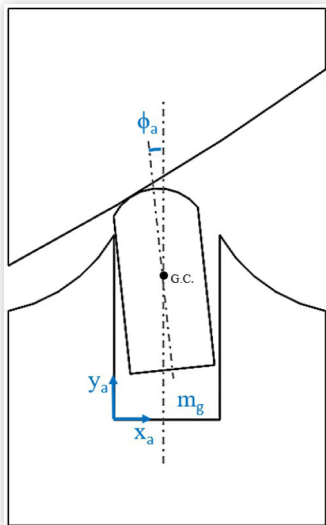
© SAE International

in which x and y are the displacement in the direction of the groove and perpendicular to the groove, ϕ is the angle of the seal and m_g is the fluid mass in the volume under the apex. All these variables are shown at Figure 7.

The error function G to be minimized to solve for X is:

$$[G] = \begin{bmatrix} F_x - ma_x \\ F_y - ma_y \\ T_\phi - ma_\phi \\ \dot{m}_g - \dfrac{\Delta m_g}{\Delta t} \end{bmatrix}$$

in which F_x and F_y are the forces acting on the seal in the direction x and y, T_ϕ is the moment applied to the seal, a_x and a_y are the acceleration of the seal in the x and y direction, α_ϕ is the angular acceleration of the seal, $\dot{m}_g$ is the time derivative of the mass of gas under the seal, Δm_g is the total mass flow rate into and from the groove and Δt is the time step used.

Forces on the Apex Seal Figure 8 represents the apex seal in its groove and a free-body diagram shows the different forces acting on the seal which are considered in the model. The principal types of forces that have been considered are the gas forces, the spring forces, the contact reaction forces and friction. Gas forces are caused by the gas pressure acting on each face the seal. Spring forces are the result of the spring load on the seal. Contact forces are caused by reaction forces when the seal is in contact with the groove. Friction forces are proportional to the contact forces and opposed to the relative motion between the parts. Simplified analytical models are used to calculate all the forces.

Contact Sub-Model The asperity contact pressure is calculated as a function of the clearance between the seal and

FIGURE 8 The forces included in the apex seal model are: a) contact, friction, and spring forces and b) gas forces
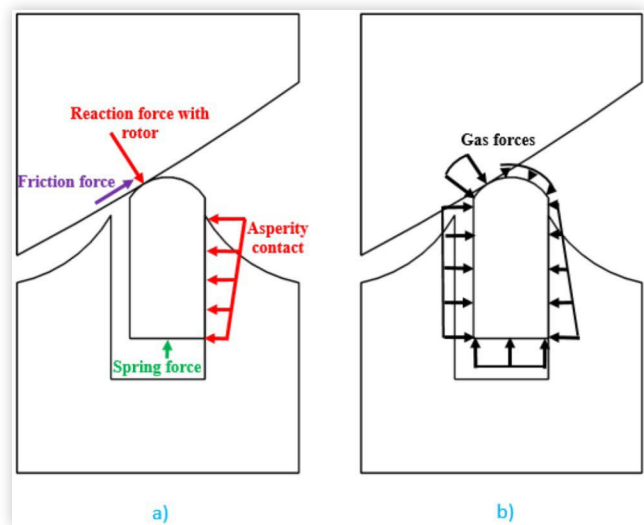
© SAE International

the groove, noted as h. The contact sub-model uses a simplified Greenwood-Tripp relation [17].

$$P_{contact} = \begin{cases} 0 & \text{for } h/\sigma_p \geq z \\ P_c \left(z - \dfrac{h}{\sigma_p} \right)^{K_c} & \text{for } h/\sigma_p < z \end{cases}$$

The Pc, z and Kc constants are taken from piston engine work by Chen [18] to represent the topography of the groove. They are respectively equal to 127 kPa, 4.8 and 6.804. The σ_p parameter represents the standard surface roughness deviation. It is set at 0.1 µm based on surface roughness measurements.

Friction between the rotor and the apex seal is calculated using the contact pressure and a friction coefficient of 0.15.

Gas Pressure & Leakage Flow The gas pressure in each chamber is measured experimentally and the resulting pressure traces are used to calculate the pressure on both side of the apex at each time step. The pressure is measured near the center of the combustion center, but is estimated to be the same in all the working chamber.

Because the gases in the channel move at a greater speed than the apex itself, the gas flow in the channels is approximated as a Poiseuille flow. The gas flow is calculated by integrating the cubic height of the channel:

$$q = -\frac{\Delta P}{12\mu \int_0^{L_c} \dfrac{1}{h^3} dx_c}$$

in which ΔP is the pressure difference at both ends of the channels, calculated using the pressure traces for the combustion chambers and the variable which represents the mass of gas under the apex seal, μ is the dynamic viscosity of the fluid, h is the height of the channel, x_c is the distance in the direction of the channel and L_c is the total length of the channel.

Knowing the fluid flow across the entire channel, the pressure distribution can be identified back using the previous relation to identify the pressure variation for each element of the channel:

$$dP = \frac{12\mu q dx_c}{h^3}$$

The gas flow is considered incompressible to calculate the pressure distribution acting on the seal, but the mass flow is limited by the maximum compressible flow allowed through an orifice with an area equivalent to the minimum section of the channel.

Oil Film Pressure Generation The hydrodynamic pressure generated by the oil film can be implemented in the model. However, based on results from the model including hydrodynamic pressure, it has little impact on the leakage values and it thus not included in this paper for the sake of simplicity. It should be noted that hydrodynamic pressure must be included to correctly predict friction power and wear.

Face Seal Model

The face seal model shares a lot of similarities with the apex seal model. The same Newton-Raphson solver is used in both models. The asperity contact function used is still based on the simplified Greenwood-Tripp relation, and the flow equations are still based on a Poiseuille flow. However, the face seal is much more flexible than the apex seal, and it would lead to false conclusions to evaluate it as a rigid body. It is therefore studied as a flexible beam.

The complex shape of the seal is approximated by curved beam elements with respective radius values. A dual-grid approach used by Baelden [19] to study the behavior of piston ring is used. This allows to use fewer structural elements and still obtains accurate results. The seal deformation is evaluated along 4 different directions, which are presented at Figure 9.

Rigidity and Mass Matrices The error function needs to include the rigidity of the seal:

$$[G] = [F] - [K][X] - [M][a]$$

in which G is the error function, F is the force vector, K is the rigidity matrix of an element, X is the variables vector, M is the mass matrix and a is the acceleration vector.

Because the section width of the seal is an order of magnitude less than the radius of curvature of the elements, the curved beams elements are treated as thin beams. The displacements are small, as the seal is constrained by the rotor.

The rigidity, mass and forces for each element are calculated using Hermite polynomials. In this model, cubic polynomial shape functions are used, which corresponds to four degrees of freedom per node. The 4 shape functions are described here, knowing that η is the angle between the beginning of a curved element and it coordinate and that Θ_e is the total angular length of the element, so that η varies from 0 to 1 throughout the element:
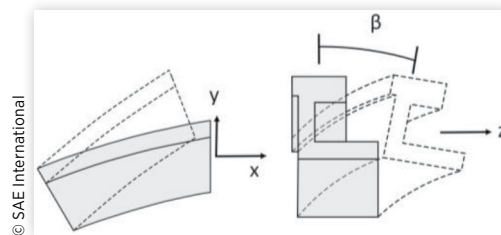
$$N_1 = 1 - 3\eta^2 + 2\eta^3$$
$$N_2 = \theta_e \left(\eta - 2\eta^2 + \eta^3 \right)$$
$$N_3 = 3\eta^2 - 2\eta^3$$
$$N_4 = \theta_e \left(-\eta^2 + \eta^3 \right)$$

In the plane of curvature, the x and y displacements are coupled together, a rigidity matrix can therefore be identified

FIGURE 9 The face seal can move in 3 different directions - circumferentially (*x*), radially (*y*), and axially (*z*) - and tilt (*β*)

for both nodes located at the beginning and at the end of the element.

$$kx_b = \begin{bmatrix} kx_{11} & kx_{12} \\ kx_{21} & kx_{22} \end{bmatrix}; \quad kx_e = \begin{bmatrix} kx_{33} & kx_{34} \\ kx_{43} & kx_{44} \end{bmatrix}$$

In which the subscript b means at the beginning of the element and e means at the end of the element.

And from the interaction of both nodes, cross-terms appear:

$$kx_{be} = \begin{bmatrix} kx_{13} & kx_{14} \\ kx_{23} & kx_{24} \end{bmatrix}; \quad kx_{eb} = \begin{bmatrix} kx_{31} & kx_{32} \\ kx_{41} & kx_{42} \end{bmatrix}$$

The subscript eb and be then means represent the cross terms between the beginning and end of the element. The axial rigidity terms can be calculated using the contribution of each degree of freedom to the deformation energy of the beam:

$$kx_{ij} = \frac{L_e}{R^2} \int_0^1 AE N_i' N_j' \, d\eta$$

in which i and j represents a number from 1 to 4, indicating the row and column it belongs to in kx, and the shape functions to use. A is the area of the cross-section of the seal, E is the Young modulus, L_e is the length of the element and R is the radius of the element. The same technique can be used to identify the relation in y:

$$ky_{ij} = \frac{L_e}{R^4} \int_0^1 EI_z \left(N_i + N_i'' \right)\left(N_j + N_j'' \right) d\eta + \frac{L_e}{R^2} \int_0^1 AE N_i N_j \, d\eta$$

in which I_z is the inertia around the z axis. The k_{xy} matrix describes the coupling between the x and y displacements, in which the same subscript logic is applied for I and j:

$$kyx_{ij} = \frac{L_e}{R^2} \int_0^1 AE N_i N_j' \, d\eta$$

in which:

$$kxy = kyx^T$$

The same logic applies to the deformation out of the plane of curvature:

$$kz_{ij} = \frac{L_e}{R^4} \int_0^1 \left(EI_y N_i'' N_j'' \, d\eta + GJ_t N_i' N_j' \right) d\eta$$

$$k\beta_{ij} = \frac{L_e}{R^2} \int_0^1 \left(EI_y N_i N_j + GJ_t N_i' N_j' \right) d\eta$$

$$kz\beta_{ij} = \frac{L_e}{R^3} \int_0^1 \left(EI_y N_i' N_j' \, d\eta - GJ_t N_i' N_j' \right) d\eta$$

$$k\beta z = kz\beta^T$$

In which I_y is the inertia around the y axis, G is the shear modulus and J_t is the torsional constant. The final rigidity matrix can then be assembled as:

$$K = \begin{bmatrix} kx_b & kxy_b & 0 & 0 & kx_{be} & kxy_{be} & 0 & 0 \\ kyx_b & ky_b & 0 & 0 & kyx_{be} & ky_{be} & 0 & 0 \\ 0 & 0 & kz_b & kz\beta_b & 0 & 0 & kz_{be} & kz\beta_{be} \\ 0 & 0 & k\beta z_b & k\beta_b & 0 & 0 & k\beta z_{be} & k\beta_{be} \\ kx_{eb} & kxy_{eb} & 0 & 0 & kx_e & kxy_e & 0 & 0 \\ kyx_{eb} & ky_{eb} & 0 & 0 & kyx_e & ky_e & 0 & 0 \\ 0 & 0 & kz_{eb} & kz\beta_{eb} & 0 & 0 & kz_e & kz\beta_e \\ 0 & 0 & k\beta z_{eb} & k\beta_{eb} & 0 & 0 & k\beta z_e & k\beta_e \end{bmatrix}$$

The mass matrix can be found using the same strategy, but applied to the kinetic energy:

$$Mx_b = \begin{bmatrix} Mx_{11} & 0 \\ 0 & Mx_{22} \end{bmatrix}; \quad Mx_e = \begin{bmatrix} Mx_{33} & 0 \\ 0 & Mx_{44} \end{bmatrix}$$

$$Mx_{be} = \begin{bmatrix} Mx_{13} & 0 \\ 0 & Mx_{24} \end{bmatrix}; \quad Mx_{eb} = \begin{bmatrix} Mx_{31} & 0 \\ 0 & Mx_{42} \end{bmatrix}$$

Which coefficients are determined by:

$$Mx_{ij} = L_e \int_0^1 \rho A N_i N_j \, d\eta$$

in which ρ is the density of the material. Knowing that the mass is an isotropic property:

$$Mx = My = Mz$$

And that the twist inertia is calculated with:

$$M\beta_{ij} = L_e \int_0^1 \rho I_p N_i N_j d\eta$$

in which I_p is the moment of inertia.

$$M = \begin{bmatrix} Mx_b & 0 & 0 & 0 & Mx_{be} & 0 & 0 & 0 \\ 0 & My_b & 0 & 0 & 0 & My_{be} & 0 & 0 \\ 0 & 0 & Mz_b & 0 & 0 & 0 & Mz_{be} & 0 \\ 0 & 0 & 0 & M\beta_b & 0 & 0 & 0 & M\beta_{be} \\ Mx_{eb} & 0 & 0 & 0 & Mx_e & 0 & 0 & 0 \\ 0 & My_{eb} & 0 & 0 & 0 & My_e & 0 & 0 \\ 0 & 0 & Mz_{eb} & 0 & 0 & 0 & Mz_e & 0 \\ 0 & 0 & 0 & M\beta_{eb} & 0 & 0 & 0 & M\beta_e \end{bmatrix}$$

The forces are calculated by integrating the forces per unit length on an element, giving the following matrices, in which v represents the degrees of freedom, x, y, z or β:

$$Fx_b = \begin{bmatrix} Fx_1 \\ Fx_2 \end{bmatrix}; \quad Fx_e = \begin{bmatrix} Fx_3 \\ Fx_4 \end{bmatrix}$$

To find the resulting forces, the load f on the beam and the shape functions can be used:

$$Fv_i = \int_0^{L_e} f_{vi} N_i ds$$

Which result can then be assembled to find the final forces vector:

$$F = \begin{bmatrix} Fx_b \\ Fy_b \\ Fz_b \\ F\beta_b \\ Fx_e \\ Fy_e \\ Fz_e \\ F\beta_e \end{bmatrix}$$

Forces on the Face Seal The face seal must resist to the same set of forces as the apex seal, with the addition of the inertial forces, due to the face seal moving with the rotor. Gas forces are mostly important on the side exposed to the working chamber. The inertial forces are calculated with the kinematics of the engine. The spring force allows constant contact between the seal and the running face, even when the pressure in the working chamber is low. Figure 10 shows an example of all the forces acting on the seal.

Modeling Results

The apex seal model is used to simulate the dynamics of the seals at 7000 rpm, the design point of the engine, and full load. The apex model predicts fast transition from one flank to the other and therefore low flank leakage. The face seal model predicts that the face seal seals relatively well in the high pressure area, but not in the low pressure area, or near the apex seals, where the face seals tends to distance itself from the rotor.

FIGURE 10 Forces acting on the face seal cross-section a) Contact, spring and friction forces b) Gas and pseudo forces
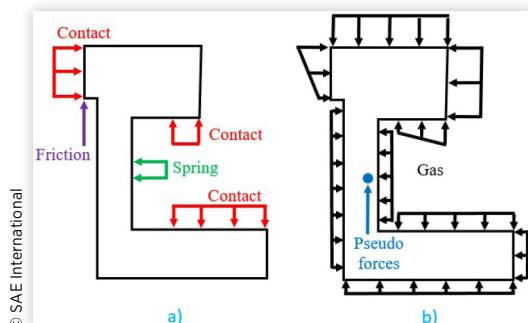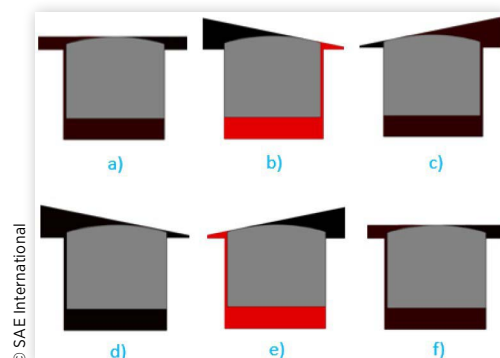

Apex Seal Model Results

The position of the seal as well as geometrical and flank leakage predicted are shown in Figure 11. Geometrical leakage follows the pressure trace, the flow being proportional to the pressure difference between the two adjacent chambers. Flank leakage is negligible compared to geometrical leakage. This is explained by the small mass of the apex seal compared to the large forces, which leads to large accelerations when one side is pressurized. The apex seal moves from one side of the groove to the other quickly in around 20 CA. Furthermore, the pressure difference between the high pressure chamber and the low pressure chamber is low when the seal is moving between the flanks. During the rest of the cycle, the apex seal remains in contact with the low pressure flank, effectively sealing the groove. This phenomenon is illustrated at Figure 12, in which the low pressure gases are black, and the high pressure gases are red. Chamber 2 is located and the left and chamber 3 is located on the right of the apex seal on the figure.

FIGURE 11 The leakage caused by the dynamics of the apex is small compared to the geometric leakage as the pressure difference is small when the apex moves from one flank to the other and remains in contact with the low pressure flank when the chamber pressure is high
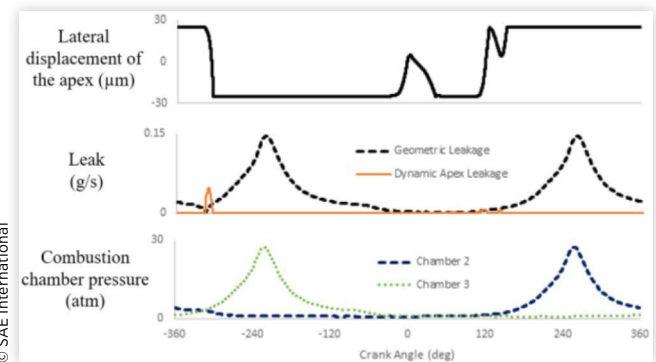

FIGURE 12 Position of the seal and chamber pressures at a) start of cycle b) TDC of chamber 3 c) expansion of chamber 3 d) compression of chamber 2 e) TDC of chamber 2 f) end of cycle

Face Seal Model Results

Under high gas pressure, the face seal conforms to the rotor and due to the one-piece design of the external face seal, minimal leakage occurs. Under low pressure, the centrifugal forces are dominant and the seal is pushed towards the exterior, and therefore does not seal as intended. However, since pressure is low in this case, the gas leaks at a slow rate. The intersection between the region where gas pressure is dominant and the region where centrifugal forces are dominant is subject to another leakage mechanism. As the pressure is high on one side of the apex and low on the other side and because the face seal is not infinitely flexible, a small portion of the face seal losses contact with the rotor near the apex in the high pressure portion, as depicted in Figure 13. The resulting leakage over a complete cycle is shown in Figure 14. It shows that leakage occurs as soon as there is a pressure difference between the chambers, but is limited when the pressure is high, because it conforms better under high pressures.

FIGURE 13 Model results show that the face seal conforms to the rotor in the high pressure zone, but lifts off in the low pressure zone. Gas pressure is illustrated in black, contact pressure is illustrated in red and blue represents the inertial forces

© SAE International
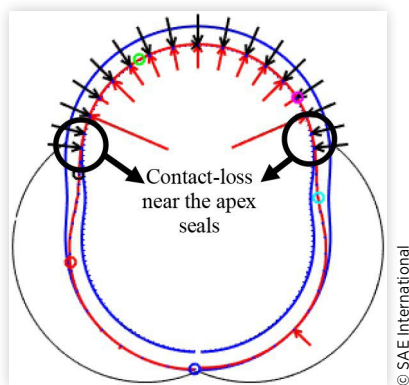
FIGURE 14 The face seal a) leaks on a good portion of the cycle, but at a relatively controlled rate b) leak mass flow is influenced by the pressure in each chamber

© SAE International
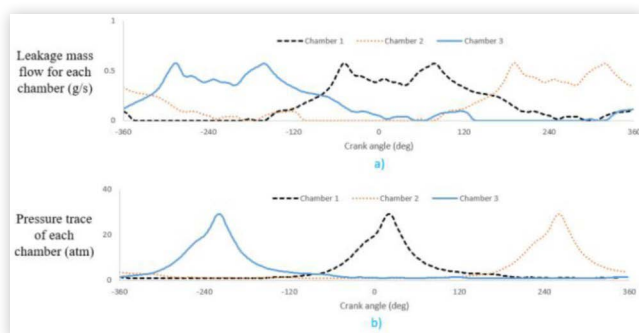
Experimental Results

Experimental tests were conducted to study the sealing performance of the X engine and validate the seals models. Figure 15 shows the dynamometer setup on which the engine ran to acquire data relative to the engine. A GT-Power model for the engine was used to determine the equivalent leakage orifice area by fitting the results to the experimental data acquired. A best fit of the data was identified at 0.8 mm^2 at 7000 rpm for the X engine.

To find the appropriate leakage value, the GT-Power model iterates the size of the equivalent orifice for each chamber and seek the value that provide the minimum error with test data. The minimum error is obtained by comparing the model data and test data values for brake power, BSFC, engine air flow rate and peak cylinder pressure, while subject to constraints such as estimates of heat transfer percentage and combustion efficiency.

Equivalent Leakage Area

The leakage from the apex seal and face seal models are converted to an equivalent leakage area, defined as the equivalent orifice area between the chamber and the atmosphere that produces the same total leakage over a complete rotor revolution. Assuming the same running face leakage as a scaled Wankel engine, the X engine total equivalent leakage area should be around 0.4 mm^2/chamber at high speed. To give an order of magnitude, the total leakage area of the Wankel engine, as developed by Mazda Motor Corporation is 2 mm^2 at 8000 rpm, based on modeling [4].

In order to compare the leakage area of the two engines, the Wankel engine is scaled down to 70 cc. The sealing mechanisms quantified by Picard et al. [4] for rotary engines are first divided in two categories: (1) leakage that depends directly on sealing length -running face, flank and spark plug leakage - and

FIGURE 15 The x engine equivalent leakage area was calculated by comparing GT-Power results and experimental data [20]

© SAE International
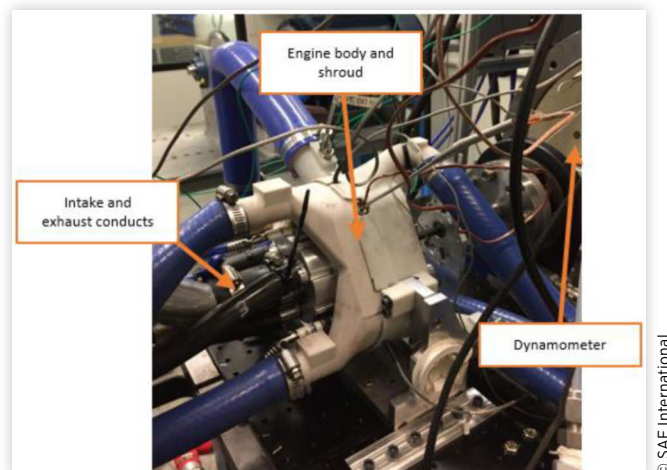
FIGURE 16 The X engine eliminates some of the most important leakage mechanisms of the Wankel by its design
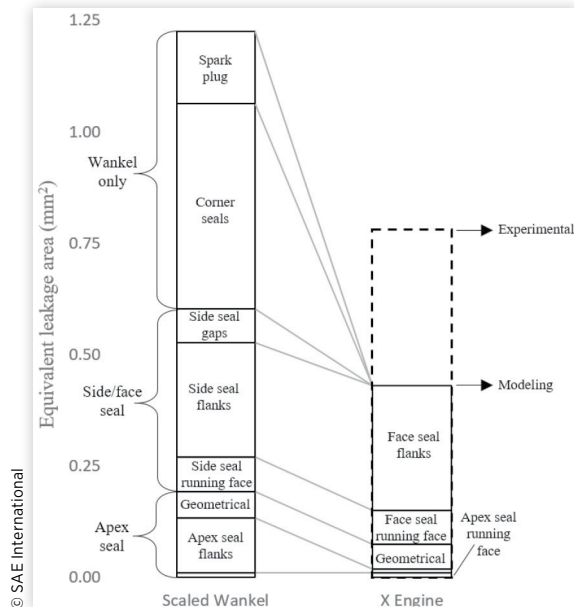
(2) geometrical leakage through the gaps between the seals and around the corner seals. Equivalent leakage area of the leakage mechanisms that depends on sealing length are scaled linearly with the total seal length. As sealing length scales with the cubic root of the volume, the 500 mm sealing length of the 650 cc Mazda engine reduces to 236 mm for a 70 cc Wankel engine. The leakage that depends on sealing length area are therefore scaled down by a factor of 2.1. Geometrical leakage areas are kept constant, independently of engine scale. The rational for this approximation is that the apex seal cross-section must remain the same to prevent increasing contact pressure in order to avoid excessive wear. If the apex seal cross-section remains the same, the corner seal also remains the same size. The side seal is also kept with the same cross-section by symmetry with the other seals. As the seals are the same, except for their length, it is assumed that the gaps between them remains the same.

The breakdown of the 70 cc X engine leakage is compared to the breakdown of a scaled 70 cc Wankel engine in Figure 16. The predicted leakage area of the X engine is about 3 times lower than that of the Wankel as corner seal and spark plug leakage are removed and face seal and apex seal leakage are kept to a reasonable amount. Removing the corner seals provides the largest benefit as it removes many gaps between seals. The second most important gain is the elimination of sparkplug leakage as the X engine apex seals are stationary and therefore do not cross the sparkplug holes during the combustion cycle.

In the Wankel engine, important leakage happens near the corner seal, because the interaction between the parts prevents the seal to conform in this area. The face seal in the X engine conforms well to the rotor edge in the area exposed to the working chamber. In the area opposed to the working chamber however, the seal is pushed on the external direction, and therefore does not seal as well, but because the pressures are low, the leaks are reasonable.

The face seal running face leakage value depends on the thermal and mechanical distortion of the face plates, which is not known at this moment for the X engine. As the distortion is expected to be similar and that leakage mechanism is relatively small, the same leakage area as the Wankel is used as an approximate value.

Apex seal flank leakage predicted is small as the apex seal remains in contact with the groove flank when pressure in the chamber is high. In the absence of body forces, there is no force to open the low pressure flank as predicted in the Wankel engine. Finally, geometrical leakage is about the same as the scaled Wankel engine and running face is approximated to be about the same as the scaled Wankel.

Summary/Conclusions

This paper shows that the presented X Engine sealing concept has the potential to achieve good sealing for a rotary engine. According to the models and to the scaling method used to compare with bigger engines, the X engine has the potential to achieve an equivalent leakage orifice size 65% lower than traditional Wankel's. The most important contributors to this reduction are the elimination of two leakage mechanisms, the corner and sparkplug gaps, along with the reduction of flank leakage for both the apex and face seals.

Leakage mechanisms for both the apex and face seals of the X engine are evaluated and quantified in this paper with detailed dynamics models that predict the position of the seals for every crank angle of the cycle and the resulting leakage. The apex seal predicted leakage is small due to their stationary position. The external face seal performs well because of its one-piece design, which allows good conformability to the rotor and limits the number of interfaces between the parts.

The experimental data fitted with a GT-Power model supports the conclusions of the model, as it already shows an equivalent leakage area about 35% lower than the leakage area of a scaled Wankel.

References

[1] L. Tartakovsky, V. Baibikov, M. Gutman, M. Veinblat, and J. Reif, "Simulation of Wankel Engine Performance Using Commercial Software for Piston Engines," SAE International, Warrendale, PA, 2012-32-0098, Oct. 2012.

[2] J. Spreitzer, F. Zahradnik, and B. Geringer, "Implementation of a Rotary Engine (Wankel Engine) in a CFD Simulation Tool with Special Emphasis on Combustion and Flow Phenomena," 2015.

[3] Picard, M., Tian, T., and Nishino, T., "Predicting Gas Leakage in the Rotary Engine-Part I: Apex and Corner Seal," *Journal of Engineering for Gas Turbines and Power* 138(6), 2016.

[4] Picard, M., Tian, T., and Nishino, T., "Predicting Gas Leakage in the Rotary Engine-Part II: Side Seals and Summary," *Journal of Engineering for Gas Turbines and Power* 138(6), 2016.

[5]   Eberle, M.K. and Klomp, E.D., "An Evaluation of the Potential Performance Gain from Leakage Reduction in Rotary Engines," SAE Technical Paper 730117, 1973.

[6]   Danieli, G.A., Ferguson, C.R., Heywood, J.B., and Keck, J.C., "Predicting the Emissions and Performance Characteristics of a Wankel Engine," SAE Technical Paper 740186, 1974.

[7]   T. J. Norman, "A Performance Model of a Spark Ignition Wankel Engine : Including the Effects of Crevice Volumes, Gas Leakage, and Heat Transfer," Master's Thesis, Massachusetts Institute of Technology, 1983.

[8]   Roberts, J.A., Norman, T.J., Ekchian, J.A., and Heywood, J.B., "Computer Models For Evaluating Premixed and Disc Wankel Engine Performance," SAE Technical Paper 860613, 1986.

[9]   Matsuura, K., Kazuo, T., and Watanabe, I., "The Behavior of a Rotary Engine Apex Seal against the Trochoidal Surface," *Bull. JSME* 21(161):1642-1651, 1978.

[10] Matsuura, K., Terasaki, K., and Watanabe, I., "The Relative Behavior of a Rotary Engine Apex Seal to the Walls of a Slot," *Bull. JSME* 19(137):1367-1375, 1976.

[11] Knoll, J., Vilmann, C.R., Schock, H.J., and Strumpf, R.P., "A Dynamic Analysis of Rotary Combustion Engine Seals," SAE Technical Paper 840035, 1984.

[12] Orlandea, N.V., Welnert, M.S., and Keleher, D.B., "Computer Simulation of the Rotary Engine Apex Seal System," SAE Technical Paper 870410, 1987.

[13] Shkolnik, A., Littera, D., Nickerson, M., Shkolnik, N., and Cho, K., "Development of a Small Rotary SI/CI Combustion Engine," SAE Technical Paper, Warrendale, PA, SAE Technical Paper 2014-32-0104, Nov. 2014.

[14] Shkolnik, N. and Shkolnik, A., "Rotary High Efficiency Hybrid Cycle Engine," *SAE Tech. Pap.*01-2448, 2008.

[15] Nabours, S., Shkolnik, N., Nelms, R., Gnanam, G., and Shkolnik, A., "High Efficiency Hybrid Cycle Engine," *SAE International, Warrendale, PA*, 2010-01-1110, Apr. 2010.

[16] Costa, T.J. et al., "Measurement and Prediction of Heat Transfer Losses on the XMv3 Rotary Engine," *SAE International Journal of Engines* 9(4):2368-2380, Nov. 2016.

[17] Greenwood, J.A. and Tripp, J.H., "The Contact of two Nominally Flat Rough Surfaces," *Proc. Inst. Mech. Eng.* 185(1):625-633, Jun. 1970.

[18] H. Chen, "Modeling the Lubrication of the Piston Ring Pack in Internal Combustion Engines Using the Deterministic Method," Ph.D. Thesis, Massachusetts Institute of Technology, 2011.

[19] C. Baelden, "A Multi-Scale Model For Piston Ring Dynamics, Lubrication and Oil Transport in Internal Combustion Engines," Ph.D. Thesis, Massachusetts Institute of Technology, 2014.

[20] Littera, D. et al., "Development of the XMv3 High Efficiency Cycloidal Engine," SAE Technical Paper, Warrendale, PA, SAE Technical Paper 2015-32-0719, Nov. 2015.

Contact Information

Maxime Leboeuf can be reached at
Maxime.Leboeuf@usherbrooke.ca

Mathieu Picard can be reached at
Mathieu.Picard@usherbrooke.ca

LiquidPiston can be reached at
info@liquidpiston.com

Acknowledgments

Definitions/Abbreviations

TDC - Top dead center
BSFC - Brake specific fuel consumption
CA - Crank angle